LIMNOLOGY and OCEANOGRAPHY

ASLO

Limnol. Oceanogr. 9999, 2022, 1–12

doi: 10.1002/lno.12232

Oceanic lobate ctenophores possess feeding mechanics similar to the impactful coastal species *Mnemiopsis leidyi*

Malaika Cordeiro,[1,a] John H. Costello ,[2,3] Brad J. Gemmell ,[4] Kelly R. Sutherland ,[5] Sean P. Colin [1,3*]

[1]Department of Marine Biology and Environmental Science, Roger Williams University, Bristol, Rhode Island
[2]Biology Department, Providence College, Providence, Rhode Island
[3]Whitman Center, Marine Biological Laboratory, Woods Hole, Massachusetts
[4]Department of Integrative Biology, University of South Florida, Tampa Bay, Florida
[5]Oregon Institute of Marine Biology, University of Oregon, Eugene, Oregon

Abstract

Lobate ctenophores are often numerically dominant members of oceanic epipelagic and midwater ecosystems. Despite this, little is known about their trophic ecology. Multiple, co-occurring species are often found in these ecosystems and appear to feed similarly via feeding currents that entrain prey. We quantified the hydrodynamics, morphology, and behavior of four co-occurring, cosmopolitan lobate species (*Eurhamphaea vexilligera*, *Ocyropsis crystallina*, *Bolinopsis vitrea*, and *Leucothea multicornis*) to evaluate whether their feeding mechanics lead to differential feeding rates and prey selection. We compared the feeding characteristics of these four oceanic species to the coastal lobate ctenophore, *Mnemiopsis leidyi*, which is known as a voracious zooplanktivore. We found that despite their morphological diversity, the five lobate species used the same mechanism to generate their feeding current—the hydrodynamics of their feeding currents were similarly laminar and with very low fluid deformation rates. Despite having similar feeding current traits, the species had different in situ swimming behaviors and feeding postures. We show that these different behaviors and postures lead to different prey encounter rates and that several of the oceanic species have the potential to feed at rates similar to or greater than *M. leidyi*. As such, the individual and combined trophic impact of oceanic lobate ctenophores is likely to be much greater than previously predicted.

The surface and mid-water regions of the world's oceans are vast and comprise the largest ecosystem in the world. These oceanic communities, including the epi- and mesopelagic realms, are dominated by gelatinous zooplankton such that food webs in these communities have been termed "Jelly Webs" (Robison 2004). Recent studies have revealed the trophic importance and complexity of these jelly webs (Choy et al. 2017; Hays et al. 2018; Chi et al. 2020). Ctenophores (or "comb jellies") are ubiquitous and often highly numerous members of these ecosystems. Despite their global distributions, there are virtually no quantitative studies examining how oceanic ctenophores function and feed. The delicate nature of oceanic ctenophores has hampered the study of these animals and their role in oceanic ecosystems.

Most oceanic ctenophores are from the orders Lobata (or lobate ctenophores) or Cydippida (Gibbons et al. 2021; Schiariti et al. 2021). Lobate ctenophores have large oral lobes, reduced tentillae, and use fused cilia (or ctenes) arranged along four auricles to generate a feeding current. Cydippid ctenophores do not have lobes but have long tentillae and generally feed by sitting motionlessly with their tentacles deployed. Feeding-current foraging by lobates increases the volume of water encountered by feeding structures and elevates their predatory impact above ambush foraging cydippids (Buecher and Gasser 1998; Colin et al. 2015). Due to their cosmopolitan distributions, abundances, and foraging strategies, lobate ctenophores have the potential to structure oceanic communities.

*Correspondence: scolin@rwu.edu

[a]Present address: CalTech, Pasadena, California

Author Contribution Statement: S.P.C., J.H.C., K.R.S., and B.J.G. collected the video in the laboratory and the field. M.C. and S.P.C. analyzed the video and the data. S.P.C. wrote the main manuscript text. All the authors reviewed the manuscript.

The vast majority of lobate ctenophore taxa occur in oceanic epi-pelagic and midwater ecosystems. However, their limited accessibility and delicate morphology have restricted quantitative studies. Observations of their swimming and feeding behavior have mostly relied upon remotely operated vehicles (ROV) and SCUBA techniques (Hamner et al. 1987; Matsumoto and Hamner 1988; Haddock 2007). However, most of our quantitative understanding of the functional biology and ecological role of lobate ctenophores comes from studies on the coastal lobate *Mnemiopsis leidyi*. *M. leidyi* has been shown to rely on two complementary feeding mechanisms (Costello et al. 1999; Waggett and Costello 1999). It produces a continuous, slow feeding current to entrain prey and transport them past their auricles. The auricles are sensory structures that scan the feeding current for prey. Sensed prey are diverted to the tentillae (Colin et al. 2010, 2015). Because the feeding current is hydrodynamically silent, mechanosensitive prey typically do not detect any fluid mechanical disturbance until they are close to the auricles. In addition, *M. leidyi* can sense and react to highly mobile, reactive copepods before they reach the auricles by closing their lobes. This behavior increases the likelihood of copepods jumping into and being captured by the lobes (Costello et al. 1999). As a result of these mechanisms, laboratory studies have shown *M. leidyi* to have very high capture efficiencies of even the most reactive copepods (> 80%; Colin et al. 2015; Costello et al. 1999).

These stealthy, efficient feeding mechanisms make *M. leidyi* a voracious predator with a greater predatory impact than most other gelatinous predators (Colin et al. 2015). Moreover, these prey capture techniques are effective even in turbulent coastal waters (Sutherland et al. 2014; Jaspers et al. 2017). Through its predation, *M. leidyi* has been implicated in the collapse of the fishing industry in the Black Sea and repeatedly has been documented to cause trophic cascades in coastal ecosystems (Daskalov et al. 2007; Dinasquet et al. 2012; Tiselius and Møller 2017).

Previous underwater observations of multiple species of oceanic lobate ctenophores indicate that oceanic lobates may use encounter and capture mechanisms similar to *M. leidyi* (Matsumoto and Hamner 1988; Matsumoto 1991; Haddock 2007). If so, these lobate ctenophores may have a greater impact than currently thought on the community structure and material cycling in oceanic communities. Strikingly, food web and carbon cycling models often do not incorporate gelatinous zooplankton. When gelatinous taxa are included in models, ctenophores and other gelatinous taxa such as medusae are not differentiated (Acuña et al. 2011; Jaspers et al. 2015; Luo et al. 2020) or ctenophores are excluded altogether owing to the dearth of data on their abundance and distribution (Wright et al. 2021).

Here, we quantified and compared the feeding current, morphology, and foraging behavior of four species of lobate ctenophores (*Eurhamphaea vexilligera*, *Ocyropsis crystallina*, *Bolinopsis vitrea*, and *Leucothea multicornis*; Fig. 1) which occur globally and are often co-occurring, dominant lobates found in epipelagic ecosystems (Harbison et al. 1978; Gibbons et al. 2021; Schiariti et al. 2021). Their feeding parameters were compared to the coastal lobate *M. leidyi* in order to determine how the foraging of oceanic ctenophores may compare to the well-studied *M. leidyi*. We addressed the following questions: (1) are auricular beat patterns and the hydrodynamics (structure, flow velocity, and fluid deformation rates) of feeding currents similar across lobate ctenophores? (2) Do flow patterns vary with feeding behavior (hovering vs. swimming)? And (3) how do in situ foraging behaviors (swimming speed, lobe postures, and morphology) compare among lobates? If oceanic species employ similar prey capture mechanisms to the coastal *M. leidyi*, their predation impact may be greater than previously realized.

Methods

Collection and maintenance of ctenophores

Data were collected using SCUBA diving techniques off Woods Hole, MA (41°31′36.7″N, 70°40′30.6″W), West Palm Beach, FL (26°43′93″ N, 79°59′15″W), and off the Kona coast

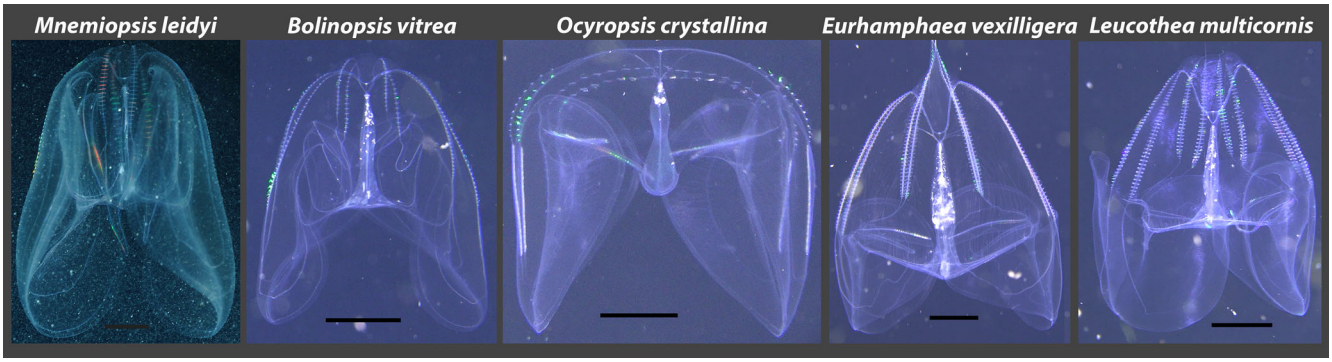

Fig. 1. In situ images of lobate ctenophore species examined in this study. *M. leidyi* is a coastal species while *B. vitrea*, *O. crystallina*, *E. vexilligera*, and *L. multicornis* are found in the epipelagic zone in oceans around the world. Scale bars are 1 cm.

of Hawaii (19°40′10.5″N, 156°02′46.4″W). Ctenophores were hand-collected by SCUBA divers using 1-L jars and laboratory work was conducted within hours of collection. Once collected, the animals were immediately transported to the laboratory for particle image velocimetry (PIV) analysis. Morphometric and behavioral data were collected using recordings from custom underwater video/imaging systems of animals in their natural environment using SCUBA techniques.

Auricular ctene kinematics

To examine whether the auricular ctenes of *B. vitrea*, *O. crystallina*, *E. vexilligera*, and *L. multicornis* use the same symplectic (power stroke of the cilia is in the same direction of the propagated wave) and dexioplectic (power stroke of cilia moves at an angle relative to the propagated wave) metachronal beat kinematics as *M. leidyi*, free swimming ctenophores were video recorded after being placed into glass rectangular vessels with collimated light directed straight into the camera lens (Colin et al. 2015). Specific metachronal kinematics can be used as an indicator of whether the auricles are functioning to simply move fluid or to process prey (Knight-Jones 1954). Auricular motions were recorded at 1000 frames per second using a Photron Fastcam mini AX200.

Particle image velocimetry

The hydrodynamics of the feeding currents generated by each species was quantified using 2D PIV. Video recordings were made of freshly caught individuals using large glass filming vessels with natural seawater that was collected along with the ctenophores (*L. multicornis* was excluded from the hydrodynamic analysis because we were unable to get them to swim and feed in the laboratory). Hollow glass PIV beads (10 μm) were added to the seawater and the vessel was illuminated using a red laser sheet (1 mm thick). The glass beads did not have a visible effect on the swimming and feeding behavior. Only sequences where the ctenophores were in their feeding posture, with lobes wide open, and with the laser sheet transecting through the middle of the animal were selected for PIV analysis. Selected image pairs were subsequently analyzed in DaVis 8.3.1 (LaVision GmbH) using a cross-correlation PIV algorithm with a decreasing interrogation window size of 64 × 64 pixels to 32 × 32 pixels or 32 × 32 pixels to 16 × 16 pixels with 50% overlap to produce velocity vectors and vorticity contours. Maximum normal strain (D) was calculated from the velocity vector fields generated in the PIV analysis using the DaVis 8.3.1 software based on the eigenvalues of the matrix:

$$\begin{pmatrix} \mathrm{E}_{xx} & E_{xy} \\ E_{yx} & E_{yy} \end{pmatrix} \quad (1)$$

where

$$d_1 = \left(E_{xx} + E_{yy}\right)/2 \quad (2)$$

$$d_2 = \sqrt{\frac{\left(E_{xx} - E_{yy}\right)^2}{4} + \frac{\left(E_{xy} - E_{yx}\right)^2}{4}} \quad (3)$$

$$D = d1 + d2 \quad (4)$$

Maximum normal strain extracts the largest component of fluid deformation which makes it a good indicator of the hydrodynamic signal produced by the feeding current that may be sensed by copepod prey. Copepod prey respond to mechanical signals when the deformation rate is greater than its threshold regardless of its direction (Kiørboe and Visser 1999; Kiørboe et al. 1999).

In situ swimming and morphometrics

The amount of fluid that the ctenophores process for encountering prey, defined as $F_{\max}$, is affected by the size of the ctenophores, how wide they open their lobes, and their swimming speed (Colin et al. 2010). These parameters were quantified by video recording undisturbed individuals in the water column using high-resolution 4K video cameras (Sony AX100) with brightfield collimated-light optical systems (Townsend et al. 2020; dx.doi.org/10.17504/protocols.io.kxygxz4ykv8j/v2). From the video, we measured the total length (T), the lobe length (l), the lobe width (w), and gap opening width (g). After passing between the lobes, the fluid passes past the beating auricles and away from the ctenophore (Colin et al. 2010, 2015). We estimated the space that the auricles occupy in the gap between the lobes as a ratio of the 2D projected space of the auricles and the total space of the opening through which the fluid exits the space between the lobes.

In situ swimming speed (U) was quantified from the videos by measuring the speed relative to ambient particles near the ctenophore. Only particles that were in plane with the ctenophore and passed between or adjacent to the lobes were selected. The volume of fluid that passed between the lobes ($F_{\max}$) of individual ctenophores in the field was calculated by multiplying their measured swimming speed (since it was much greater than the feeding current velocity) by their measured area of the lobe opening. This area (*see* Fig. 5E) was approximated as an ellipse with the length and width equaling their measured lobe width (w) and gap opening width (g), respectively:

$$F_{\max} = \mathrm{U}(1/4\mathrm{wg}\pi) \quad (5)$$

To examine how their encounter rates may change with size for the total range of sizes (total length = T) observed for each population we calculated a theoretical $F_{\max}$ using Eq. 5

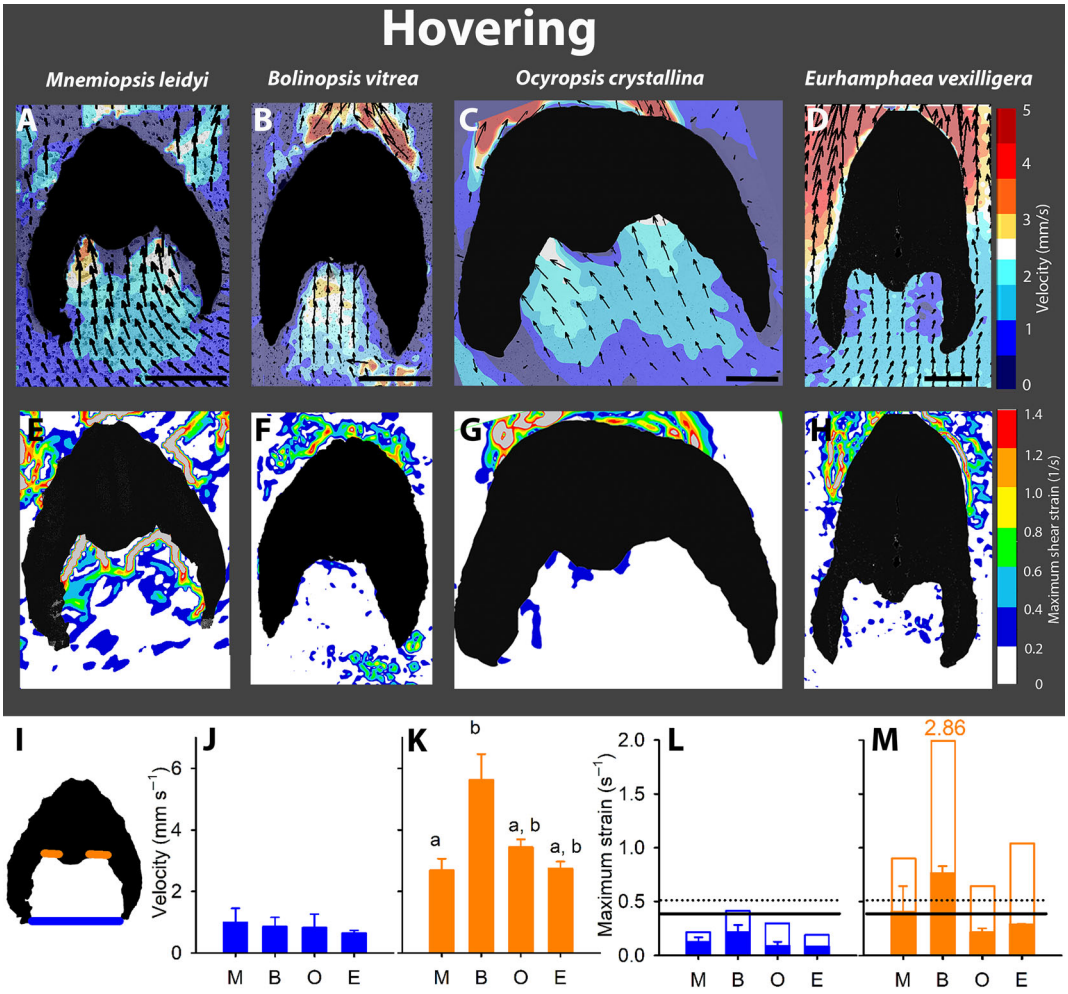

Fig. 2. Hydrodynamics of lobate ctenophores while hovering. (**A**–**D**) Velocity vectors and contours and (**E**–**H**) maximum strain rate contours around the different lobate species (black bars = 1 cm). (**I**) Schematic of transects over which the velocities and deformation rates were averaged for each species. Blue and orange colors correspond to values from the lobe tips and auricles, respectively. Average fluid velocities (n = 3 ctenophores per species) at the (**J**) lobe tips and the (**K**) auricles. Maximum strain rates at the (**L**) lobe tips and the (**M**) auricles (filled and open bars show the average and maximum strain values across the transect measured). Dashed and solid lines indicate detection thresholds of copepods *Acartia tonsa* (Kiørboe et al. 1999) and *Tortanus* sp. (Burdick et al. 2007), respectively.

where U was the average swimming speed for each species and w and g were based on the morphometric ratios for each species (*see* Fig. 4A,B) multiplied by a range of total lengths (T).

The raw data used in this study are publicly available and can be found at: https://www.bco-dmo.org/project/776095

Statistical analysis

Statistical analyses were performed using SigmaPlot v13 statistical software. ANOVA tests were performed to compare the flow and morphology among species. Holm–Sidak tests were used to make post-hoc comparisons (significance level, $\alpha = 0.05$). If the data did not conform to the assumptions of homoscedasticity (Browne–Forsythe test) and normality (Shapiro–Wilk test) then the non-parametric Kruskal–Wallis one-way ANOVA on ranks test was used for comparisons.

For comparisons of shear deformation between hovering and swimming ctenophores, the data among species were pooled because they did not differ statistically and a T-test was used to compare the pooled data.

Regressions of size vs. clearance rates (F_{max}) for the five ctenophore species were compared using an analysis of covariance (ANCOVA) using SigmaPlot v13 statistical software. Data were checked for their agreement with the assumptions of normality, equal variances, and equal slopes.

Results

Auricular ctene kinematics

The auricles of all the oceanic ctenophore species examined, *B. vitrea*, *O. crystallina*, *E. vexilligera*, and *L. multicornis*

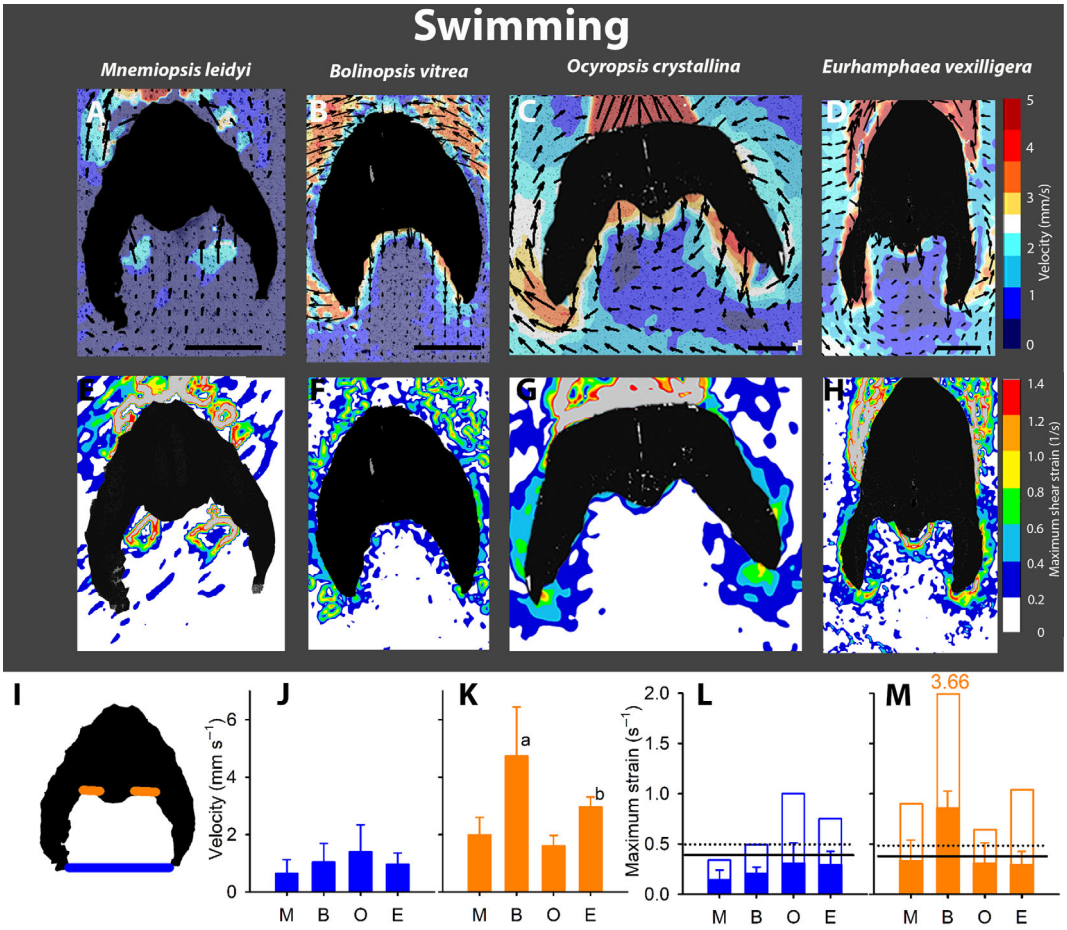

Fig. 3. Hydrodynamics of lobate ctenophores while swimming. (**A**–**D**) Velocity vectors and contours and (**E**–**H**) maximum strain rate contours around the different lobate species (black bars = 1 cm). (**I**) Schematic of transects over which the velocities and deformation rates were averaged for each species. Blue and orange colors correspond to values from the lobe tips and auricles, respectively. (**J**–**M**) Average fluid velocities ($n = 3$ ctenophores per species) at the (**J**) lobe tips and the (**K**) auricles. Maximum strain rates at the (**L**) lobe tips and the (**M**) auricles (filled and open bars show the average and maximum strain rates across the transect measured). Dashed and solid lines indicate detection thresholds of copepods *Acartia tonsa* (Kiørboe et al. 1999) and *Tortanus* sp. (Burdick et al. 2007), respectively.

used the same type of metachronal beat kinematics as has been described for *M. leidyi* (Colin et al. 2015) to generate their feeding current. This beat pattern differs from that of the ctene rows, which are used for propulsion. Ctene rows that run along the outside of the lobes are known to beat with an antiplectic (power stroke of the cilia is in the opposite direction of the propagated wave) metachronal wave, while high-speed video demonstrated that the auricular cilia have both symplectic (power stroke of the cilia is in the same direction of the propagated wave) and dexioplectic components (power stroke of cilia moves at an angle relative to the propagated wave).

Feeding current hydrodynamics

In the laboratory, the ctenophores were observed in their feeding stance creating a feeding current with their lobes in a wide-open position. They were observed in this stance while both hovering (swimming velocity = 0) and swimming (swimming velocity > 0). *B. vitrea*, *O. crystallina*, and *E. vexilligera* produced a feeding current with a similar structure (i.e., paths the flow takes around the ctenophores) and with similar hydrodynamic characteristics to *M. leidyi*. In both modes, fluid was pulled between the lobes then over the auricles and away from the ctenophore (Figs. 2, 3). While hovering, the flow of all the species was very slow at the lobe tips (< 2 mm s^{-1}, ANOVA, $n = 3$ or 4 inds, df = 3, $F = 0.364$, $p = 0.8$) and accelerated as it approached the auricles where it peaked before being transported outside the lobes. The maximum flow velocities at the auricles differed significantly among species (ANOVA, $n = 3$ or 4 inds, df = 3, $F = 28.6$, $p = 0.002$) and flows were faster for *B. vitrea* than *M. leidyi* and *E. vexilligara* (Holm–Sidak post-hoc analysis, $p < 0.05$). The mean maximum

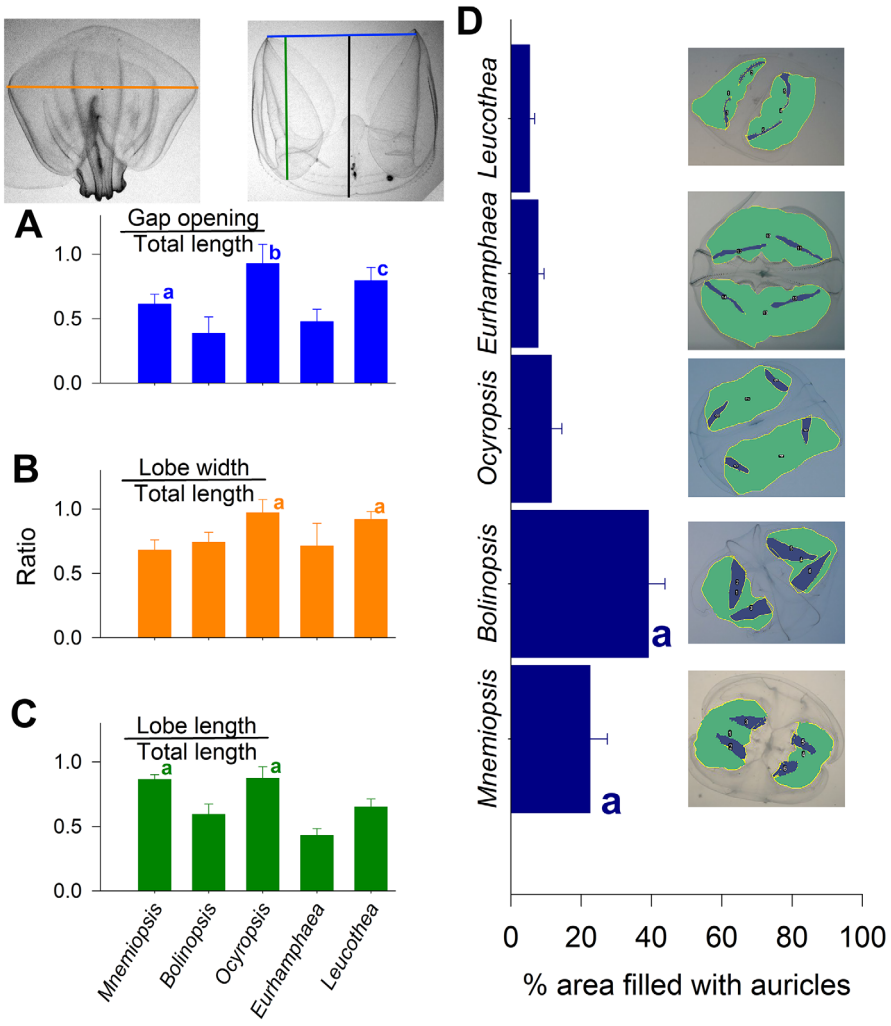

Fig. 4. In situ morphometrics of the lobate ctenophores: *M. leidyi* ($n = 12$), *B. vitrea* ($n = 8$), *O. crystallina* ($n = 10$), *E. vexilligera* ($n = 10$), and *L. multicornis* ($n = 9$). (**A–C**) Lobe and opening size relative to the ctenophore's total length. The distances measured for each are indicated by the color of the bars and the corresponding line in the images of *Ocyropsis crystalina*. (**D**) Percent of the exit area filled by the auricles. Higher percentages correspond to the feeding current needing to be more confined between the auricles and the lobes as it exits the ctenophore.

strain rates (averaged across the opening) were also very low at the lobe tips (≤ 0.2 s^{-1}) and did not vary significantly among species (Kruskal–Wallis ranks test $p > 0.05$). As reference points, we have plotted the deformation detection limits of two species of copepods (i.e., *Tortanus* sp. (Fig. 2, solid line) and *Acartia* sp. (Fig. 2, dashed line); Kiørboe et al., 1999; Burdick et al. 2007). Both copepods are coastal species and, while neither are known to co-occur with the ctenophores examined, they are two of the most sensitive copepod species described in the literature and are shown as reference points. As such, the maximum strain rates observed at the lobe tips were below or just at the detection limits of these most sensitive copepods. Higher observed deformation values only occurred in proximity to the lobe surfaces (due to the boundary layer) and most of the lobe openings had much lower deformation values than the maximum values (Fig. 2). The deformation was greatest near the auricles with maximum values greater than the detection limit of copepods.

The hydrodynamics of the feeding current while swimming were similar to hovering with a similar structure and similarly low velocities at the lobe tips (< 2 mm s^{-1}, Fig. 2; *T*-test comparing hover vs. swim velocities at lobes for pooled data among species, $n = 14$, $p = 0.7$). The primary difference was that deformations rates around the lobe tips were greater during swimming due to the "bow wave" around the tips (Fig. 2; *T*-test comparing hover vs. swim deformation rates at lobes for pooled data among species, $n = 14$, $p = 0.004$). As a result, the region of flow that was below the detection limit of the most sensitive copepods would be smaller for swimming ctenophores than hovering ctenophores. As with hovering, maximum deformation levels at the auricles during swimming were above the detection limits of copepod prey.

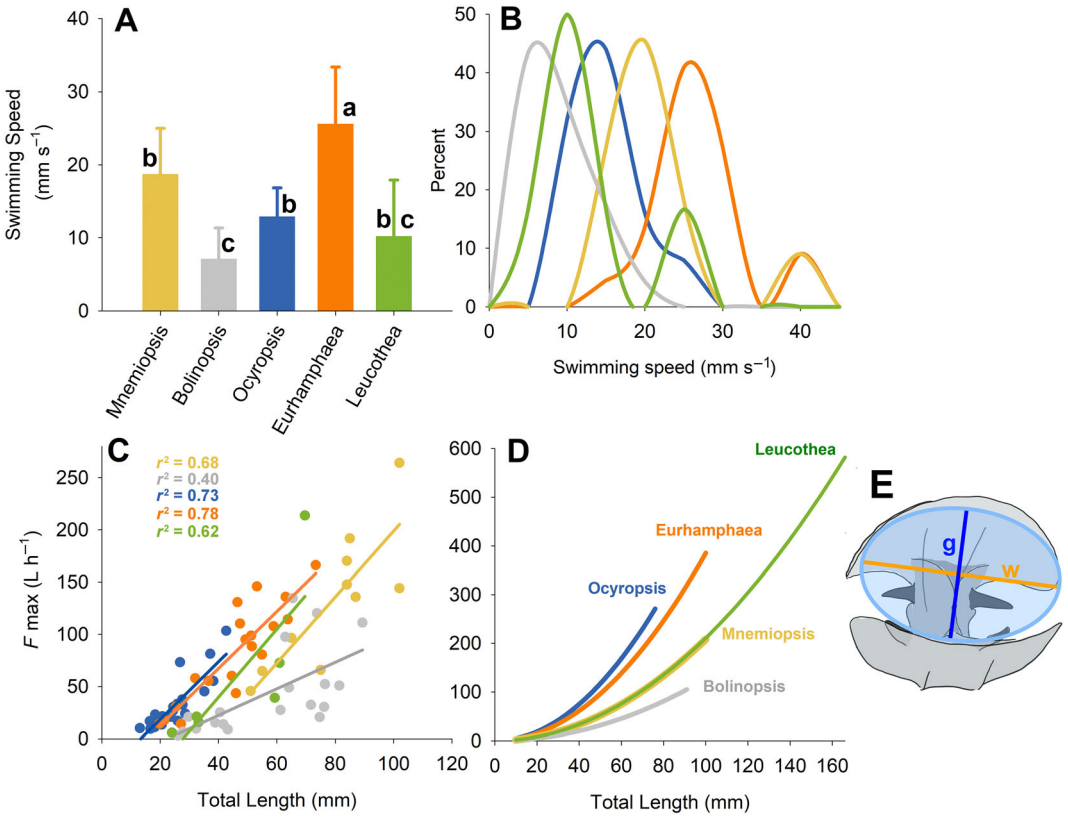

Fig. 5. In situ swimming speeds and maximum clearance rates (F_{max}) by lobate ctenophores. (**A**) Mean swimming speeds (± SD) for *M. leidyi* ($n = 11$, yellow), *B. vitrea* ($n = 24$, gray), *O. crystallina* ($n = 25$, blue), *E. vexilligera* ($n = 22$, orange), and *L. multicornis* ($n = 6$, green). (**B**) Frequency distribution of observed swimming speeds. (**C**) In situ flux rates of feeding current into the lobe volume (i.e., F_{max}) vs. ctenophore length based on each individual's swimming speed, gap opening and lobe width. (**D**) Modeled F_{max} vs. ctenophore size based on in situ swimming speeds and mean gap width and lobe width from Fig. 4a,b. The maximum lengths modeled were based on the maximum ctenophore length (T) that we observed in the field. (**E**) Schematic of measurements made to calculate ellipse used to estimate F_{max}.

In situ lobe morphology and positioning

While the feeding current characteristics among the lobate species were similar, predator–prey interactions are also influenced by variations in body size, morphology, and lobe positioning. To examine the lobe morphology and positioning, we compared the ratios of lobe width, length, and opening to total ctenophore length among the species. Unlike hydrodynamic measurements, the lobe morphologies and positioning observed in the field differed among species (Fig. 4A). The body of *O. crystallina* almost completely consisted of their lobes (with lobe length/total and width/total being close to 1). In addition, they were observed in the field with their lobes positioned the furthest apart—a configuration that increases their encounter volume (Fig. 4A, Holm–Sidak post-hoc comparison, $p < 0.05$). *L. multicornis* was also observed with their lobes more open than *M. leidyi*, *E. vexilligera*, and *B. vitrea* (Fig. 4A, Holm–Sidak post-hoc comparison, $p < 0.05$). And *M. leidyi* swam with their lobes more open than *B. vitrea* and *E. vexilligera* and their lobes extended most of their total length. In contrast, *B. vitrea* and *E. vexilligera* were observed with their lobes closer together and their lobes made up a smaller proportion of their total body.

Auricle morphology

We compared the spacing around the auricles because the confinement of the flow as it passes the auricles may impact the ability of the auricles to sensory scan prey. The feeding current of *M. leidyi* and *B. vitrea* becomes more confined as it passes their auricles because the auricles filled up more of the space through which the fluid must pass (≥ 25% of the area, Holm–Sidak post-hoc comparison, $p < 0.05$). In contrast, the auricles of *L. multicornis*, *O. crystallina*, and *E. vexilligera* filled < 10% of the flow area resulting in less constriction of the fluid as it passes the auricles.

In situ swimming behavior and encounter rates (F_{max})

If in situ swimming speeds are greater than feeding current velocities (Figs. 2, 3) then prey encounter rates will ultimately be determined by swimming behavior (Colin et al. 2015). In situ quantification of swimming showed that the different species swim at different speeds (Fig. 5A,B). *E. vexilligera* swam

the fastest, averaging about 26 mm s^{-1}, with fastest individuals swimming at more than 40 mm s^{-1}. *M. leidyi* and *O. crystallina* swam slower than *E. vexilligera* but faster than *B. vitrea*, which swam at speeds < 10 mm s^{-1}. Interestingly, swimming speeds were not significantly related to total length for any of the species (regression analysis, $p > 0.1$). It is also important to note that variances were relatively small within each species, indicating that all the species that we encountered were swimming (and not hovering) at speeds close to their observed mean.

The volume flux that passes between the lobes is an estimate of the ctenophore encounter rates (F_{max}) and was estimated by multiplying the observed swimming velocity (U) by the area through which the fluid passes between the lobes (Fig. 5C). The F_{max} increased with size for all the species (regression analysis, $p < 0.005$). Analysis of covariance among species was performed and when *B. vitrea* was included, the slopes violated the equal slopes assumption of the test (ANCOVA equal slopes test, $p < 0.05$). Figure 5C revealed that the slope of *B. vitrea* was most different from the other four species. To test if the slopes of the other four species were equal and if their y-intercepts were similar, *B. vitrea* was excluded from the analysis. The slopes of the other four species were not significantly different (ANCOVA equal slopes test, $p = 0.7$) but the regressions were significantly different (ANCOVA, df = 3, $p = 0.002$). Post-hoc analysis revealed that the F_{max} (y-intercept) for *M. leidyi* was significantly lower than both *O. crystallina* and *E. vexilligera* (post-hoc analysis Holm–Sidak method, $p < 0.05$).

The measured F_{max} values in Fig. 5C were only from a limited size range of individuals based on the size range that we had all the necessary measurements for an individual (i.e., swimming speed [U], lobe width [w], and gap width [g]). However, much smaller and larger individuals occur in each ctenophore population. Therefore, to examine how an F_{max} may vary across the complete range of ctenophore sizes that occurred in the population for each species we calculated a theoretical F_{max} based on mean swimming speed multiplied and average morphometrics for each species (Fig. 4A,B). Swimming speed was constant for each species because, as mentioned above, we found that speed did not differ significantly with size for any of the ctenophore species (regression, $p > 0.1$). If swimming speed is assumed to be constant, then F_{max} increases as a square function of length (since the area of the opening is a square function of size) (Fig. 5D). Large *L. multicornis* and *E. vexilligera* are predicted to have the

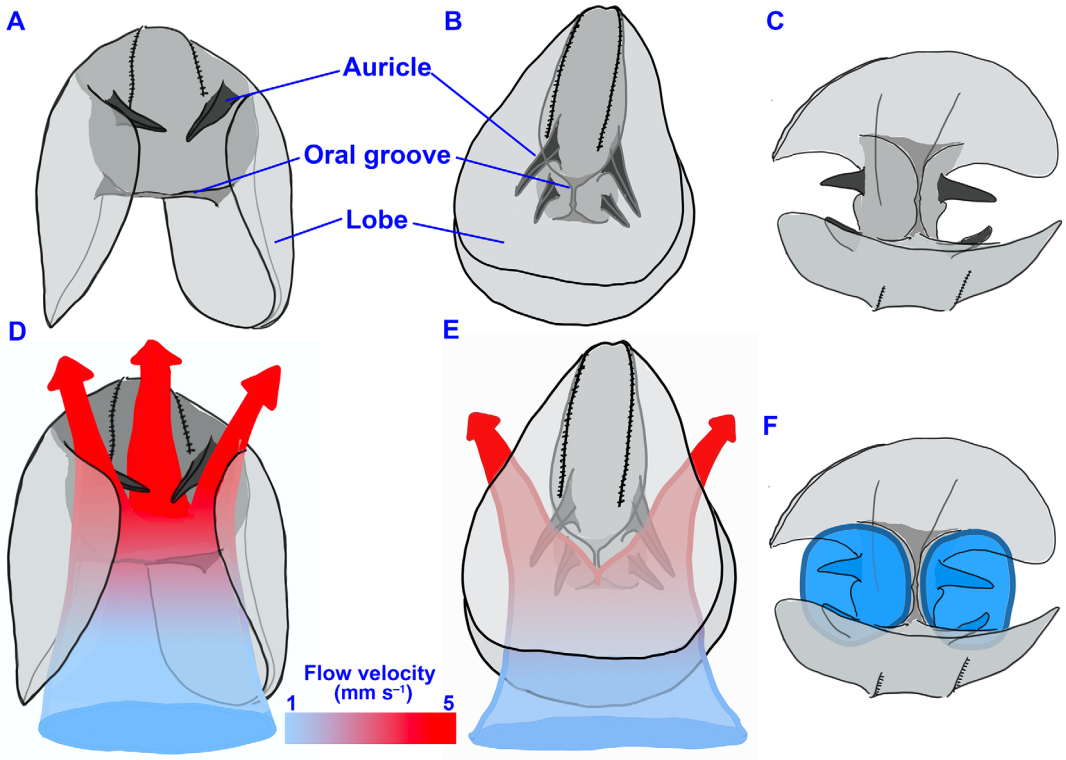

Fig. 6. Schematic of generic body and feeding current structures shared by lobate ctenophores. (**A**–**C**) Different views of simplified body morphology of lobate ctenophores consisting of two lobes (light gray) connected by central body and oral groove (medium gray). Four auricles protrude from the body between the lobes (dark gray) which have beating ctenes that generate and direct the feeding current. (**D, E**) Different views of how the feeding current travels between the lobes and accelerates and travels around the auricles before exiting the lobe volume. (**F**) View of the region through which the feeding current is constricted as it passes the sensory auricles.

highest F_{max} values since they are the largest ctenophores that we observed in situ.

Discussion

The common coastal lobate ctenophore *M. leidyi* encounters and captures prey with stealth and efficiency and is well documented as an impactful predator (Costello et al. 2006; Daskalov et al. 2007; Dinasquet et al. 2012; Tiselius and Møller 2017). Feeding current hydrodynamics, behavior, lobe morphology and sensory capabilities are key components to the successful feeding strategy of *M. leidyi*. Here, we found that the common oceanic lobate species examined rely on similar feeding current hydrodynamics, behavior, and morphology. Their similarities suggest that oceanic species have the potential to feed as efficiently and substantially as the coastal *M. leidyi*. Interestingly, encounter rates (F_{max}) based on observed in situ swimming speeds are 10 times greater than encounter and feeding rates measured from laboratory studies suggesting that lobate ctenophores may not capture prey under natural conditions as efficiently as in the laboratory (Costello et al. 1999; Waggett and Costello 1999).

Shared feeding current characteristics

Hydrodynamics, morphology, and sensory abilities collectively influence prey encounter and capture. Morphologically, lobate ctenophores appear highly complex because of their unique body plans. The key morphological features are remarkably consistent across species, which process fluid in a similar and efficient manner (Fig. 6). All lobates have two broad lobes (Fig. 6, light gray) that are joined by the central body (Fig. 6, medium gray) with the mouth ridge that joins the two lobes. Projected out from each side of the central body (between the lobes) are two auricles (Fig. 6, dark gray) that are lined with comb rows. The auricular comb rows beat with a unique symplectic metachronal pattern that differs from the antiplectic pattern of the ctene rows. This metachronal patterns is thought to aid in processing particles (Knight-Jones 1954). Sharing the same metachronal kinematics suggests that the lobates investigated in this study use the auricles to process and sense prey similarly.

The beating auricular ctenes generate the feeding current, and our data indicate that the feeding currents of the three oceanic lobates examined have the same basic structure and characteristics as *M. leidyi*. The fluid of all the feeding currents traveled slowly between the lobes and accelerated as it approached the beating ctenes on the auricles (Figs. 2, 3, 6). The flow then traveled over the mouth ridge, past the auricles, and away from the ctenophores (Fig. 6). The prey encounter rate (F_{max}) depends on the speed and volume of fluid passing between the lobes. Interestingly, we found that all the species swam faster than the fluid velocities generated by feeding currents (Fig. 5). Therefore, for ctenophores in the field, swimming speed should determine how fast the fluid passes between the lobes.

All the species examined create minimal water disturbances (measured as shear deformation rates) at their lobe tips (i.e., the entrance to their encounter volume between the lobes). Reactive zooplankton prey, such as copepods, use fluid deformation to detect mechanical disturbances generated by predators (Kiørboe et al. 1999). The most sensitive copepods examined can detect and react to deformation rates as low as 0.4 s^{-1} (Kiørboe et al. 1999; Burdick et al. 2007). Mechanosensitive prey transported between the lobes should not be able to detect any of the lobate ctenophores until they approach the auricles where deformation rates rapidly increased to levels above the detection limits of copepod. However, by this time, prey are surrounded by the lobes. Observations of prey encounters with lobates indicate that reactive prey commonly respond with an escape jump when they approach the auricles and jump into the inner lobe surface to be captured (Matsumoto and Hamner 1988; Costello et al. 1999; Haddock 2007). The quiescent environment between the lobes (created by the laminar feeding current) may also aid in the detection of prey because the lobes block out environmental noise and create a region of high signal to noise allowing lobates to sense even slight disturbances.

In situ encounter rates

Encounter rates with prey (F_{max}) estimated by multiplying in situ swimming speeds by the area through which the fluid passes reveal that *O. crystallina*, *E. vexilligera*, and *L. multicornis* can process fluid and potentially encounter prey at greater rates then *M. leidyi*. Increased prey encounter rates may be an adaptation necessary for living in a prey-dilute, oceanic environment. However, the encounter rates (F_{max}) also suggest that all of the ctenophores examined encounter prey at rates 10–100 times greater than clearance rate estimates based on laboratory and in situ feeding studies of lobate ctenophores (Kremer et al. 1986*a*; Reeve et al. 1989; Båmstedt and Martinussen 2015; Jaspers et al. 2017). This suggests that the high estimates of capture efficiencies ($\sim$ 80%) by lobate ctenophores, based primarily on laboratory studies with *M. leidyi* (Costello et al. 1999; Colin et al. 2015), may be over estimates of lobate capture efficiencies in the field environment. An important consequence of encounter rates being so much greater than observed clearance rates is that differences in post-encounter ctenophore-prey interactions may be important determinates of differences in clearance rates and prey selection patterns among lobate species. Therefore, different morphologies of capture surfaces (e.g., auricles, lobes, and tentillae) and sensory capabilities will lead to different trophic roles and impacts.

Our estimates of encounter rates (Fig. 5D) are based upon observed in situ swimming speeds and the rate that fluid passes between the lobes. These values are greater than previous F_{max} estimates of *M. leidyi* based upon laboratory PIV (Colin

et al. 2010). However, laboratory estimates of F_{max} measure the rates that the auricles move and process fluids during hovering behavior. We show that the flow generated by the auricles (Figs. 2K, 3K) is up to 10 times slower than the in situ swimming speeds. Therefore, encounter rates based on swimming speeds will be much greater than those based upon auricular flow. When the ctenophores are in the field swimming rapidly it is unclear how the flow around the auricles differs from what we observed in the laboratory. In situ PIV techniques are required better understand how ctenophores process flow while swimming at speeds up to 4 cm s^{-1}.

We predict that encounter rates increase as a square of ctenophore length scale (Fig. 5D). If so, large ctenophores should have a proportionately greater trophic impact than smaller individuals. The largest lobate ctenophores encountered in oceanic environments are *L. multicornis*, having observed lengths > 20 cm (Harbison et al. 1978; and *Cestum veneris*, commonly called Venus Girdle ctenophore, which was not included in this study). The population size structure of lobate ctenophores has not been studied systematically, therefore, at this time, we do not know the potential importance of these largest ctenophores on the trophic impact of lobate communities.

Differential prey selection

Despite the hydrodynamic similarities, differences in feeding patterns have been described for the different lobate species (Matsumoto and Harbison 1993). Rather than feeding current characteristics, different feeding patterns among lobates likely arise from different morphologies and sensory capabilities. We found that among species examined, the main differences in the basic body plan described in Fig. 6 were the lobe sizes relative to the body, lobe position during swimming, and auricle morphology. While measuring prey selection was beyond the scope of the present study, it is worth considering how the different observed morphologies, in conjunction with lobe position and swimming speeds, may influence how the different species interact with prey. Lobe positioning, for example, could vary depending on food availability or be a trait that varies among populations.

Two primary capture surfaces have been described for lobates each using different mechanisms to initiate captures, the tentillae, and inner lobe surfaces (Matsumoto and Harbison 1993; Waggett and Costello 1999; Colin et al. 2015). *M. leidyi* uses sensory scanning to sense and divert less reactive prey into the tentillae (Colin et al. 2015). As such, the auricles of *M. leidyi* are broad structures that occupy a relatively large proportion of the space through which the feeding current passes (Fig. 4D). This prey selection mode is useful for the eutrophic environments where *M. leidyi* is most common and may enable it to pick out high-quality prey in high prey environments. However, the oceanic species examined occur in oligotrophic environments where retaining prey may be more important than distinguishing prey types. Three of the species examined (*O. crystallina*, *E. vexilligera*, and *L. multicornis*) have much reduced auricles that occupy only a small portion of the space through which the feeding current passes. This morphology would constrain the feeding current less at the fast swimming speeds observed in the field, however, it may be less effective at sensory scanning since the auricles are interacting with less of the feeding current. As such, we hypothesize that these species rely less on sensory scanning but rather on using their auricles to startle motile prey into their inner lobe capture surface. This has been described as a primary mechanism for *Ocyropsis* spp. and *Eurhamphaea* (Matsumoto and Hamner 1988; Matsumoto and Harbison 1993; Haddock 2007). As a result, we would expect these species to feed on more motile, large prey. Few studies have examined the prey selection by these oceanic species; however, *Ocyropsis* spp. has been shown to primarily feed on copepods caught on the inner lobe surface (Potter 2021). *Bolinopsis* spp., on the other hand, has significantly smaller lobes and broad auricles that fill the region through which the feeding current exits. The small lobes may limit their ability to retain fast, reactive prey while their broad auricles and slower swimming speeds may facilitate sensory scanning less reactive prey. Prey selection of *Bolinopsis* spp. support this hypothesis with small cladocerans and copepods, nauplii, and eggs commonly most abundant in the guts of *Bolinopsis* spp. (Nagabhushanam 1959; Kremer et al. 1986*b*; Scriven 2022). Differences in lobe and auricle morphology which result in different feeding patterns may lead to niche separation and enable different lobate species to co-occur as they are often observed doing in epipelagic ecosystems (Harbison et al. 1978; Gibbons et al. 2021).

Ecosystem implications

Potential clearance rate estimates based on swimming speeds and morphology indicate that the lobate species occurring in oceanic ecosystems around the world have the potential to remove prey at rates similar to the impactful lobate, *M. leidyi*. Predation impact will be amplified by the combined effect of co-occurring lobate species. Since few clearance rate estimates exist for oceanic ctenophores, they are currently lumped with cnidarians (siphonophores, hydromedusae, and scyphomedusae) and cnidarian estimates are commonly used for carbon cycling models (Luo et al. 2020; Wright et al. 2021). However, *M. leidyi* has been shown to have considerably higher clearance rates and trophic impact than medusae (Colin et al. 2015), and as a result, using medusae clearance rate estimates may greatly underestimate the trophic role of oceanic ctenophores. Population clearance rates will depend on ctenophore abundances and size distribution of individuals in the population (Fig. 5). Unfortunately, there is scant data on the abundances and size distribution of ctenophores in oceanic ecosystems. Improved feeding rate and population abundance data are required to effectively understand and model the trophic role of oceanic ctenophores. The hydrodynamics, swimming behavior, and morphology

described here indicate that renewed efforts to properly document ctenophore abundance and distribution are warranted based on their substantial impact on both trophic ecology and carbon cycling in oceanic ecosystems.

Data availability statement

The datasets generated during and/or analyzed during the current study are available from the corresponding author upon request.

References

Acuña, J. L. J. L., Á. López-Urrutia, and S. P. Colin. 2011. Faking giants: The evolution of high prey clearance rates in jellyfishes. Science **333**: 1627–1629. doi:10.1126/science.1205134

Båmstedt, U., and M. B. Martinussen. 2015. Ecology and behavior of *Bolinopsis infundibulum* (Ctenophora; Lobata) in the Northeast Atlantic. Hydrobiologia **759**: 3–14. doi:10.1007/s10750-015-2180-x

Buecher, E., and B. Gasser. 1998. Estimation of predatory impact of *Pleurobrachia rhodopis* (cydippid ctenophore) in the northwestern Mediterranean Sea: In situ observations and laboratory experiments. J. Plankton Res. **20**: 631–651. doi:10.1093/plankt/20.4.631

Burdick, D. S., D. K. Hartline, and P. H. Lenz. 2007. Escape strategies in co-occurring calanoid copepods. Limnology **52**: 2373–2385. doi:10.2307/4502387

Chi, X., and others. 2020. Tackling the jelly web: Trophic ecology of gelatinous zooplankton in oceanic food webs of the eastern tropical Atlantic assessed by stable isotope analysis. Limnol. Oceanogr. **1–17**: 289–305. doi:10.1002/lno.11605

Choy, C. A., S. H. D. Haddock, and B. H. Robison. 2017. Deep pelagic food web structure as revealed by in situ feeding observations. Proc. R. Soc. B Biol. Sci. **284**: 20172116. doi:10.1098/rspb.2017.2116

Colin, S. P., J. H. Costello, L. J. Hansson, J. Titelman, and J. O. Dabiri. 2010. Stealth predation and the predatory success of the invasive ctenophore *Mnemiopsis leidyi*. Proc. Natl. Acad. Sci. USA **107**: 1–5. doi:10.1073/pnas.1003170107

Colin, S. P., R. MacPherson, B. Gemmell, J. H. Costello, K. Sutherland, and C. Jaspers. 2015. Elevating the predatory effect: Sensory-scanning foraging strategy by the lobate ctenophore *Mnemiopsis leidyi*. Limnol. Oceanogr. **60**: 100–109. doi:10.1002/lno.10007

Costello, J. H., R. Loftus, and R. Waggett. 1999. Influence of prey detection on capture success for the ctenophore *Mnemiopsis leidyi* feeding upon adult *Acartia tonsa* and *Oithona colcarva* copepods. Mar. Ecol. Prog. Ser. **191**: 207–216.

Costello, J. H., B. K. Sullivan, D. J. Gifford, D. Van Keuren, and L. J. Sullivan. 2006. Seasonal refugia, shoreward thermal amplification, and metapopulation dynamics of the ctenophore *Mnemiopsis leidyi* in Narragansett Bay, Rhode Island. Limnol. Oceanogr. **51**: 1819–1831. doi:10.4319/lo.2006.51.4.1819

Daskalov, G. M., A. N. Grishin, S. Rodionov, and V. Mihneva. 2007. Trophic cascades triggered by overfishing reveal possible mechanisms of ecosystem regime shifts. Proc. Natl. Acad. Sci. USA **104**: 10518–10523. doi:10.1073/pnas.0701100104

Dinasquet, J., and others. 2012. Cascading effects of the ctenophore *Mnemiopsis leidyi* on the planktonic food web in a nutrient-limited estuarine system. Mar. Ecol. Prog. Ser. **460**: 49–61. doi:10.3354/meps09770

Gibbons, M. J., S. H. D. Haddock, G. I. Matsumoto, and C. Foster. 2021. Records of ctenophores from South Africa. **9**: e10697. doi:10.7717/peerj.10697

Haddock, S. H. D. 2007. Comparative feeding behavior of planktonic ctenophores. Oceans **1–7**: 847–853. doi:10.1093/icb/icm088

Hamner, W. M., S. W. Strand, G. I. Matsumoto, and P. P. Hamner. 1987. Ethological observations on foraging behavior of the ctenophore *Leucothe*a sp. in the open sea. Limnol. Oceanogr. **32**: 645–652. doi:10.4319/lo.1987.32.3.0645

Harbison, G. R., L. P. Madin, and N. R. Swanberg. 1978. On the natural history and distribution of oceanic ctenophores. Deep-Sea Res. **25**: 233–256. doi:10.1016/0146-6291(78)90590-8

Hays, G. C., T. K. Doyle, and J. D. R. Houghton. 2018. A paradigm shift in the trophic importance of jellyfish? Trends Ecol. Evol. **33**: 874–884. doi:10.1016/j.tree.2018.09.001

Jaspers, C., J. L. Acuña, and R. D. Brodeur. 2015. Interactions of gelatinous zooplankton within marine food webs. J. Plankton Res. **37**: 985–988. doi:10.1093/plankt/fbv068

Jaspers, C., J. H. Costello, K. R. Sutherland, B. Gemmell, K. N. Lucas, J. Tackett, K. Dodge, and S. P. Colin. 2017. Resilience in moving water: Effects of turbulence on the predatory impact of the lobate ctenophore *Mnemiopsis leidyi*. Limnol. Oceanogr. **63**: 445–458. doi:10.1002/lno.10642

Kiørboe, T., E. Saiz, and A. W. Visser. 1999. Hydrodynamic signal perception in the copepod *Acartia tonsa*. Mar. Ecol. Prog. Ser. **179**: 97–111.

Kiørboe, T., and A. W. Visser. 1999. Predator and prey perception in copepods due to hydromechanical signals. Mar. Ecol. Prog. Ser. **179**: 81–95.

Knight-Jones, E. W. 1954. Relations between metachronism and the direction of ciliary beat in Metazoa. J. Cell Sci. **95**: 503–521. doi:10.1242/jcs.s3-95.32.503

Kremer, P., M. F. Canino, and R. W. Gilmer. 1986*a*. Metabolism of epipelagic tropical ctenophores. Mar. Biol. **90**: 403–412. doi:10.1007/BF00428564

Kremer, P., M. R. Reeve, and M. A. Syms. 1986*b*. The nutritional ecology of the ctenophore *Bolinopsis vitrea*: Comparisons with *Mnemiopsis mccradyi* from the same region. J. Plankton Res. **8**: 1197–1208. doi:10.1093/plankt/8.6.119

Luo, J. Y., R. H. Condon, C. A. Stock, C. H. Lucas, K. A. Pitt, and R. K. Cowen. 2020. Gelatinous zooplankton-mediated

carbon flows in the global oceans: A data-driven modeling study. Global Biogeochem. Cycles **34**: e2020GB006704. doi:10.1029/2020GB006704

Matsumoto, G. I. 1991. Swimming movements of ctenophores, and the mechanics of propulsion by ctene rows. Hydrobiologia **216**: 319–325. doi:10.1007/BF00026481

Matsumoto, G. I., and W. M. Hamner. 1988. Modes of water manipulation by the lobate ctenophore *Leucothea* sp. Mar. Biol. **97**: 551–558.

Matsumoto, G. I., and G. R. Harbison. 1993. In situ observations of foraging, feeding, and escape behavior in three orders of oceanic ctenophores: Lobata, Cestida, and Beroida. Mar. Biol. **117**: 279–287. doi:10.1007/BF00345673

Nagabhushanam, A. K. 1959. Feeding of a ctenophore, *Bolinopsis infundibulum* (O. F. Müller). Nature **184**: 829. doi:10.1038/184829a0

Potter, E. (2021). Ubiquitous yet inconspicuous: Quantifying trophic impact of a widespread oceanic comb jelly (ctenophore). MSc thesis, Univ. of South Florida.

Reeve, M. R., M. A. Syms, and P. Kremer. 1989. Growth dynamics of a ctenophore (Mnemiopsis) in relation to variable food supply, I . Carbon biomass, feeding, egg production, growth and assimilation efficiency. J. Plankton Res. **11**: 535–552. doi:10.1093/plankt/11.3.535

Robison, B. H. 2004. Deep pelagic biology. J. Exp. Mar. Bio. Ecol. **300**: 253–272. doi:10.1016/j.jembe.2004.01.012

Schiariti, A., and others. 2021. Overview of the comb jellies (Ctenophora) from the South-western Atlantic and Sub Antarctic region (32–60°S; 34–70°W). New Zealand J. Marine Freshw. Res. **55**: 286–310. doi:10.1080/00288330.2020.1775660

Scriven, V. 2022. Quantitative assessment of the trophic ecology of the oceanic ctenophore, *Bolinopsis infundibulum*, in Monterey Bay, California. Master's thesis, Univ. of South Florida.

Sutherland, K. R. R., J. H. H. Costello, S. P. P. Colin, and J. O. O. Dabiri. 2014. Ambient fluid motions influence swimming and feeding by the ctenophore *Mnemiopsis leidyi*. J. Plankton Res. **36**: 1310–1322. doi:10.1093/plankt/fbu051

Tiselius, P., and L. F. Møller. 2017. Community cascades in a marine pelagic food web controlled by the non-visual apex predator *Mnemiopsis leidyi*. J. Plankton Res. **39**: 271–279. doi:10.1093/plankt/fbw096

Townsend, J. P., B. J. Gemmell, K. R. Sutherland, S. P. Colin, and J. H. Costello. 2020. Ink release and swimming behavior in the oceanic ctenophore *Eurhamphaea vexilligera*. Biol. Bull. **238**: 206–213. doi:10.1086/709504

Waggett, R. J., and J. H. Costello. 1999. Capture mechanisms used by the lobate ctenophore, *Mnemiopsis leidyi*, preying on the copepod *Acartia tonsa*. J. Plankton Res. **21**: 2037–2052.

Wright, R. M., C. Le Quéré, E. Buitenhuis, S. Pitois, and M. J. Gibbons. 2021. Role of jellyfish in the plankton ecosystem revealed using a global ocean biogeochemical model. Biogeosciences **18**: 1291–1320. doi:10.5194/bg-18-1291-2021

Acknowledgments

This work was funded by the National Science Foundation (1829913 awarded to Sean P. Colin, 1829932 awarded to Kelly R. Sutherland, 1830015 awarded to John H. Costello, and 1829945 awarded to Brad J. Gemmell).

Conflict of Interest

None declared.

Submitted 27 June 2022
Revised 29 August 2022
Accepted 04 September 2022

Associate editor: Kelly J. Benoit-Bird